POD-GALERKIN REDUCED ORDER MODEL OF THE BOUSSINESQ APPROXIMATION FOR BUOYANCY-DRIVEN ENCLOSED FLOWS

KELBIJ STAR[1,2*], GIOVANNI STABILE[3], SOKRATIA GEORGAKA[4], FRANCESCO BELLONI[1], GIANLUIGI ROZZA[3], AND JORIS DEGROOTE [2]

Abstract. A parametric Reduced Order Model (ROM) for buoyancy-driven flow is developed for which the Full Order Model (FOM) is based on the finite volume approximation and the Boussinesq approximation is used for modeling the buoyancy. Therefore, there exists a two-way coupling between the incompressible Boussinesq equations and the energy equation. The reduced basis is constructed with a Proper Orthogonal Decomposition (POD) approach and to obtain the Reduced Order Model, a Galerkin projection of the governing equations onto the reduced basis is performed. The ROM is tested on a 2D differentially heated cavity of which the side wall temperatures are parametrized. The parametrization is done using a control function method. The aim of the method is to obtain homogeneous POD basis functions. The control functions are obtained solving a Laplacian function for temperature. Only one full order solution was required for the reduced basis creation. The obtained ROM is stable for different parameter sets for which the temperature difference between the walls is smaller than for the set in the FOM used for the POD basis creation. Then, the relative error between the FOM and the ROM for temperature is below 10^{-4} and for velocity below 10^{-1} for the vast part of the simulation time. Finally, the ROM is about 20 times faster than the FOM run on a single processor.

1. Introduction

Within the MYRRHA (Multi-purpose hYbrid Research Reactor for High-tech Applications) project, the Belgian Nuclear Research Centre SCK·CEN is developing and designing an experimental fast-spectrum irradiation facility featuring a compact pool-type primary cooling system operating with molten Lead-Bismuth Eutectic. With regard to the thermal-hydraulic design and safety assessment of the reactor, a major challenge is characterizing the complex three-dimensional transport phenomena in the coolant flow field, e.g. local flow mixing, buoyancy and thermal stratification in the cold and hot plenum of the primary vessel. These phenomena may impact the system response to operational and accidental transients, such as loss of flow, on the short- and long-term. In accident conditions and after reactor shut-down, decay heat is removed

[1]SCK·CEN, Institute for Advanced Nuclear Systems,Boeretang 200, 2400 Mol, Belgium.

[2]Ghent University, Department of Flow, Heat and Combustion Mechanics, Sint-Pietersnieuwstraat 41, B-9000 Ghent, Belgium

[3]SISSA, International School for Advanced Studies, Mathematics Area, mathLab Trieste, Italy.

[1]Imperial College London, Department of Mechanical Engineering, London, SW7 2BX, UK.

E-mail addresses: kelbij.star@sckcen.be, gstabile@sissa.it, s.georgaka16@imperial.ac.uk, francesco.belloni@sckcen.be, grozza@sissa.it, Joris.Degroote@UGent.be.

Key words and phrases. proper orthogonal decomposition; finite volume approximation; reduced order modeling, POD: Proper Orthogonal Decomposition, Galerkin projection, finite volume.

*Corresponding Author.

passively via natural circulation. However, the development of the flow, for instance thermal stratification at low flow conditions, during the transition from forced to natural circulation may have a detrimental effect on the efficiency of the passive residual heat removal. Therefore, reliable computational methods are required to accurately quantify naturally circulating flows and the associated transient phenomena. [1]
One-dimensional best-estimate system thermal-hydraulic (STH) codes are usually used for reactor transient safety analyses, but have their limitations associated with the aforementioned phenomena and representation of complex flows. On the other hand, three-dimensional computational fluid dynamics (CFD) flow solvers that are based on discretization methods, of which the finite volume (FV) method is commonly used by commercial software and open-source codes, are used widely in industry to solve complex flows. However, performing transient simulations using a full numerical approach is completely unfeasible due to the excessive amount of computational resources needed, especially when a large number of different system configurations are to be tested. Also the gain in computational speed of a STH/CFD coupled model is still too limited. Therefore, model reduction techniques that have been developed to approximate the (parametrized) Partial Differential Equations (PDEs) describing the fluid problem are needed to reduce the computational effort. Moreover, a two-way coupling between momentum and energy is required to model the complex dynamics of natural circulation. Therefore, the Boussinesq approximation is often applied to simplify the problem by neglecting the effect of local density differences of the fluid, induced by temperature, except for the influence of the gravitational body force on the flow. This approximation is valid as long as the difference in density is much smaller than the reference density.
The purpose of this work is to develop a parametric Reduced Order Model (ROM) with a FV-based POD-Galerkin method for buoyancy-driven enclosed flows and is an extension of the work on a ROM for weakly coupled Navier-Stokes equations with the heat equation performed in [2].

2. Full Order Model

The mathematical problem on which this work is focused is given by the unsteady incompressible Navier-Stokes equations, without any turbulence treatment, in the presence of the gravity body force and the energy equation. The general form of the equations is

$$
\begin{cases}
\frac{\partial \rho \boldsymbol{u}}{\partial t} + \nabla \cdot (\rho \boldsymbol{u} \otimes \boldsymbol{u}) - \nabla \cdot (\mu \nabla \boldsymbol{u}) = -\nabla p + \rho \boldsymbol{g} & \text{in } \Omega, \\
\frac{\partial \theta}{\partial t} + (\nabla \cdot \boldsymbol{u})\theta - \nabla \cdot (\alpha \nabla \theta) = 0 & \text{in } \Omega, \\
\nabla \cdot \boldsymbol{u} = 0 & \text{in } \Omega, \\
\boldsymbol{u}(\boldsymbol{x}, t) = 0 & \text{on } \Gamma, \\
\theta(\boldsymbol{x}, t) = f(\boldsymbol{x}) & \text{on } \Gamma, \\
\boldsymbol{u}(\boldsymbol{x}, 0) = \boldsymbol{u}_0(\boldsymbol{x}) = \boldsymbol{g}(\boldsymbol{x}) & \text{in } \Omega, \\
\theta(\boldsymbol{x}, 0) = \theta_0(\boldsymbol{x}) = k(\boldsymbol{x}) & \text{in } \Omega,
\end{cases}
\tag{2.1}
$$

where $\boldsymbol{u}$ is the velocity, p the pressure, θ the temperature, ρ the density, μ is the dynamic viscosity, α is thermal diffusivity and $\boldsymbol{g}$ the gravitational acceleration.
The Boussinesq approximation assumes that ρ is constant for all terms in Equation. 2.1, except for the gravitational term. To avoid numerical issues due to large gradients of the buoyancy force, buoyant flow solvers typically use $p'_{rgh} = p - \rho \boldsymbol{g} \cdot \boldsymbol{r}$, with $\boldsymbol{r}$ the position vector, rather than the static pressure p. The momentum equations with the

Boussinesq approximation are then given by

$$\frac{\partial \boldsymbol{u}}{\partial t} + \nabla \cdot (\boldsymbol{u} \otimes \boldsymbol{u}) - \nabla \cdot (\nu \nabla \boldsymbol{u}) = -\nabla p_{rgh} \ - (\boldsymbol{g} \cdot \boldsymbol{r}) \nabla \rho_k, \tag{2.2}$$

where $p_{rgh} = (p - \rho \boldsymbol{g} \cdot \boldsymbol{r}) / \rho_0$ is referred to as a pressure shift and $\rho_k = 1 - \beta(\theta - \theta_0)$ with β the thermal expansion coefficient. The reference state is taken at p_0, ρ_0 and θ_0.

3. POD-Galerkin Reduced Order Model

The Proper Orthogonal Decomposition (POD) method is used to create a set of basis functions containing the essential dynamics of the previously described Full Order Model (FOM). The main assumption of POD is that the system's dynamics are governed by a reduced number of dominant modes, N_r, which are orthogonal to each other [3], $\langle \boldsymbol{\varphi}_i, \boldsymbol{\varphi}_j \rangle_{L^2(\Omega)} = \delta_{ij}$. Here $\langle \cdot, \cdot \rangle_{L^2(\Omega)}$ is the L^2 inner product of the functions over the domain Ω. These modes can be obtained by solving an eigenvalue problem [4, 5] on snapshots which are generated by sampling the FOM at several moments in time. Then it is assumed that there exists an approximation of the problem, so that the FOM can be expressed as a linear combination of orthogonal spatial modes multiplied by time-dependent coefficients. For the velocity and temperature, the approximations are given by

$$\boldsymbol{u}(\boldsymbol{x}, t) \approx \boldsymbol{u_r}(\boldsymbol{x}, t) = \sum_{i=1}^{N_r} \boldsymbol{\varphi}_i(\boldsymbol{x}) a_i(t), \qquad \theta(\boldsymbol{x}, t) \approx \theta_r(\boldsymbol{x}, t) = \sum_{i=1}^{N_r} \xi_i(\boldsymbol{x}) c_i(t), \tag{3.1}$$

where $\boldsymbol{\varphi}$ and ξ are the modes of the velocity and temperature, and respectively a and c the corresponding time-depending coefficients. To obtain a Reduced Order Model, the POD is then combined with the Galerkin projection, for which the full order system is projected onto the reduced subspace of POD modes and the difference between the FOM solution and the approximated one is minimized [6]. For more details about POD and Galerkin projection methods the reader is referred to [2, 4, 5].
For the Boussinesq approximation, special attention is paid to the Galerkin projection of the shifted pressure term, which is given by

$$\langle \boldsymbol{\varphi}_i, \nabla p_{rgh} \rangle_{L_2(\Omega)} = \int_\Omega \boldsymbol{\varphi}_i \cdot \nabla p_{rgh} d\boldsymbol{x} = -\int_\Omega p_{rgh} \left(\nabla \cdot \boldsymbol{\varphi}_i \right) d\boldsymbol{x} + \int_{\partial\Omega} p_{rgh} \left(\boldsymbol{\varphi}_i \cdot \boldsymbol{n} \right) ds. \tag{3.2}$$

Both terms, on the right hand side, are zero as the POD modes, defined as a linear combination of snapshots, preserve the divergence free property of the flow field [6] in the first term and in case of enclosed flow, the velocity is zero at the wall in the second term. The resulting ROM is then given by

$$\begin{cases} \boldsymbol{M_r} \dot{\boldsymbol{a}} - \nu \boldsymbol{B_r} \boldsymbol{a} + \boldsymbol{a}^T \boldsymbol{C_r} \boldsymbol{a} + \boldsymbol{H_r} \boldsymbol{c} = 0, \\ \boldsymbol{W_r} \dot{\boldsymbol{c}} - \alpha \boldsymbol{Y_r} \boldsymbol{c} + \boldsymbol{a}^T \boldsymbol{Q_r} \boldsymbol{c} = 0, \end{cases} \tag{3.3}$$

where

$$\begin{aligned} M_{r_{ij}} = \langle \boldsymbol{\varphi}_i, \boldsymbol{\varphi}_j \rangle_{L_2(\Omega)}, B_{r_{ij}} = \langle \boldsymbol{\varphi}_i, \Delta \boldsymbol{\varphi}_j \rangle_{L_2(\Omega)}, C_{r_{ijk}} = \langle \boldsymbol{\varphi}_i, \nabla \cdot (\boldsymbol{\varphi}_j, \boldsymbol{\varphi}_k) \rangle_{L_2(\Omega)}, \\ H_{r_{ij}} = \langle \boldsymbol{\varphi}_i, (\boldsymbol{g} \cdot \boldsymbol{r}) \nabla (1 - \beta(\xi_j - \theta_0)) \rangle_{L_2(\Omega)}, \\ W_{r_{ij}} = \langle \xi_i, \xi_j \rangle_{L_2(\Omega)}, Y_{r_{ij}} = \langle \xi_i, \Delta \xi_j \rangle_{L_2(\Omega)}, Q_{r_{ijk}} = \langle \xi_i, \nabla \cdot (\boldsymbol{\varphi}_j, \xi_k) \rangle_{L_2(\Omega)}. \end{aligned} \tag{3.4}$$

The initial conditions for the ROM are given by

$$a_i(\boldsymbol{x}, 0) = \langle \boldsymbol{\varphi}_i, \boldsymbol{u}_0(\boldsymbol{x}) \rangle_{L^2(\Omega)}, \qquad c_i(\boldsymbol{x}, 0) = \langle \xi_i, \theta_0(\boldsymbol{x}) \rangle_{L^2(\Omega)} \tag{3.5}$$

4. Non-homogeneous boundary conditions

In a POD-based ROM, the non-homogeneous BCs are, in general, not satisfied by the ROM, as the basis functions, and similarly their BCs, are a linear combination of the snapshots. Furthermore, the BCs are not explicitly present in the reduced system and therefore they cannot be parametrized directly. In literature [7], two common methods for handling the BCs are: the control function- and the penalty method. The aim of the control method is to homogenize the POD BCs [7, 4], while the penalty method enforces the BCs in the ROM with a penalty factor [7, 8]. Both methods have their own advantages and drawbacks. As the control functions are physically based, unlike the penalty factor, which is an arbitrary value, the control function method is applied here. The method is explained for the temperature BCs, although it can be applied similarly to the velocity fields.
With the control function method, the snapshots are made homogeneous by subtracting suitable control function(s) on which then the POD is performed. The result is a set of modes with homogeneous BCs. The function to be chosen is system specific. However, there are two constraints the control function has to satisfy. Firstly, the control function must be divergence free in order to retain the divergence-free property of the basis functions. Secondly, the function needs to satisfy the remaining BCs of the FOM. One way to generate a control function, $\theta_c(\boldsymbol{x})$, satisfying both constraints, is by solving a system, as close as possible to the full order system, where the boundary of interest is set to 1 and everywhere else to 0. Then the snapshots can be modified as follows

$$\theta'(\boldsymbol{x},t) = \theta(\boldsymbol{x},t) - \sum_{k=1}^{N_{BC}} \Theta_{BC}^{k}\theta_c^{k}(\boldsymbol{x}), \tag{4.1}$$

where N_{BC} is the number of non-homogeneous BCs, Θ_{BC} is the value of the boundary condition and θ_c is the control function. Then the POD is applied to these homogeneous snapshots as described previously and finally the temperature field is approximated with

$$\theta_r(\boldsymbol{x},t) = \sum_{k=1}^{N_{BC}} \Theta_{BC}^{k}\theta_c^{k}(\boldsymbol{x}) + \sum_{i=1}^{N_r} \xi_i(\boldsymbol{x})c_i(t), \tag{4.2}$$

which satisfies the boundary conditions of the problem. Θ_{BC} can be parametric. For more details on the control function the reader may take a look at [2, 4].

5. Numerical set-up

In this study, a simple configuration for natural convection is studied that consists of a 2D square enclosed cavity with differentially heated walls opposite of each other. The simulations are carried out on a square domain of length $L = 0.1$ m on which a (100 x 100) uniform mesh is constructed. A sketch of the geometry is depicted in Figure 1.
The initial temperature, θ_0, and velocity are 300 K and (10^{-4},0) m/s, respectively. The properties are taken for air with thermal diffusivity, $\alpha = \nu \ / \ Pr = 1.4{\cdot}10^{-5}$ m^2/s, kinematic viscosity $\nu = 1{\cdot}10^{-5}$ m^2/s and $Pr = 0.71$. Furthermore, the coefficient of thermal expansion, β, is $3{\cdot}10^{-3}$ K^{-1}. The left boundary is kept at the hot temperature, θ_h, and the right boundary at the cold temperature, θ_c, with $\theta_h > \theta_c$. Four parameter sets are considered for the temperature BCs, which are listed in Table 1. The unsteady governing equations are iteratively solved by the FV method with the *buoyantBoussinesqPimpleFoam* solver of the open source C++ library OpenFOAM [9]. The PIMPLE algorithm is used for the pressure-velocity coupling [10]. For

both the full- and reduced order simulations, the time discretization is treated using a backward differencing scheme.

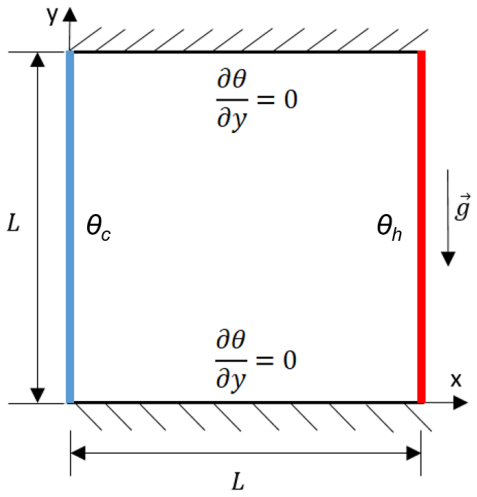

FIGURE 1. A sketch of the geometry of the 2D square cavity with differentially heated walls.

TABLE 1. Parameter sets for the temperature BCs.

Parameter set #	θ_c [K]	θ_h [K]
0	298.5	301.5
1	299.0	301.0
2	298.0	302.0
3	298.7	301.2

A constant time step of $\Delta t = 1 \cdot 10^{-3}$ s has been applied and the simulation time is 10 s. Snapshots of the velocity and temperature fields are collected every 0.01 s, resulting in a total of 1000 snapshots for each parameter set. The full order simulations are performed in OpenFOAM 6, while the Reduced Order Model is solved with ITHACA-FV, a C++ library based on the finite volume solver OpenFOAM. For more details on the ITHACA-FV code, the reader is referred to [4, 5, 11].
A control function, for each non-homogeneous BC, is determined by solving a steady state Laplacian function for temperature, $\Delta\theta = 0$, according to the methodology described in Section 4. Finally, the relative L^2-error between the FOM, X^{FOM}, and ROM fields, X^{ROM}, is determined by

$$\|e\|_{L^2}(t) = \frac{\|X^{FOM}(t) - X^{ROM}(t)\|_{L^2}}{\|X^{FOM}(t)\|_{L^2}}, \tag{5.1}$$

for both the velocity and temperature fields at each time instance, t.

6. RESULTS

First, a full order simulation is performed for parameter set 0. In total, 1000 velocity and temperature snapshots are collected. Furthermore, the control functions are obtained by solving the steady state Laplacian function and are shown in figure 2. These

functions are then used to homogenize the snapshots and to create homogeneous basis functions with the POD method.

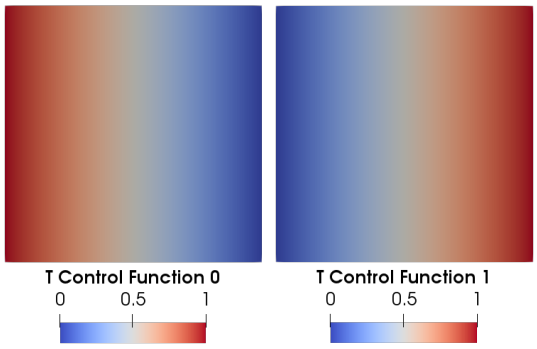

FIGURE 2. The control functions for temperature.

To determine the number of basis functions needed for the creation of the reduced subspace, the cumulative eigenvalues are plotted in Figure 3 on the left. The plot shows that 7 modes are sufficient to retain 99.9% of the energy contained in the snapshots, for both velocity and temperature.
Furthermore, the full order snapshots are projected onto the POD basis for a range of modes, from 1 to 15, to obtain time-dependent coefficients that are then used to reconstruct the fields, called the basis projection. For each number of modes the time-averaged relative L^2-error between the FOM and the basis projection is calculated and plotted in Figure 3 in the middle and on the right side for velocity and temperature, respectively.

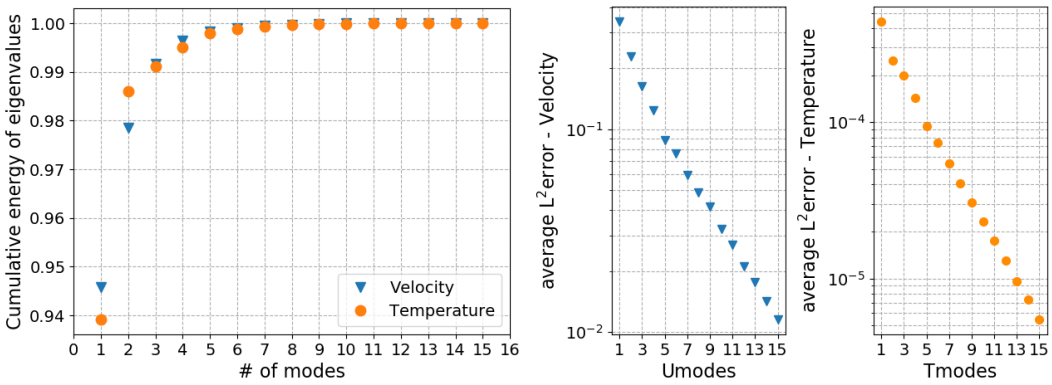

FIGURE 3. (Left) cumulative eigenvalues for velocity and temperature. (Right) the time-averaged L^2 error per number of velocity (Umodes) and temperature modes (Tmodes).

It can be seen that the slope of the decay of the time-averaged relative L^2 error for the velocity is the same as for the temperature. However, the Figure 3 shows that 5 basis functions are required to have a truncation error less than 10^{-4} for temperature, while for velocity, 5 basis functions are needed to have an error less than 10^{-1}.
The first five velocity and homogenized temperature modes are plotted in Figure 4. The velocity magnitude modes have a symmetric pattern. Furthermore, the first velocity mode is close to the steady state solution of the problem, while the first temperature

mode looks like a fluctuation around the mean field due the homogenization by the control functions. Finally, taking also into account previous observation based on the cumulative energy of the eigenvalues, 7 velocity and 7 homogeneous temperature modes are used for the reduced basis creation. Then, the ROM matrices are calculated and the obtained ROM is tested for all parameter sets. The evolution in time of the relative L^2 error between the reconstructed fields and the full order solutions is plotted in Figure 5.

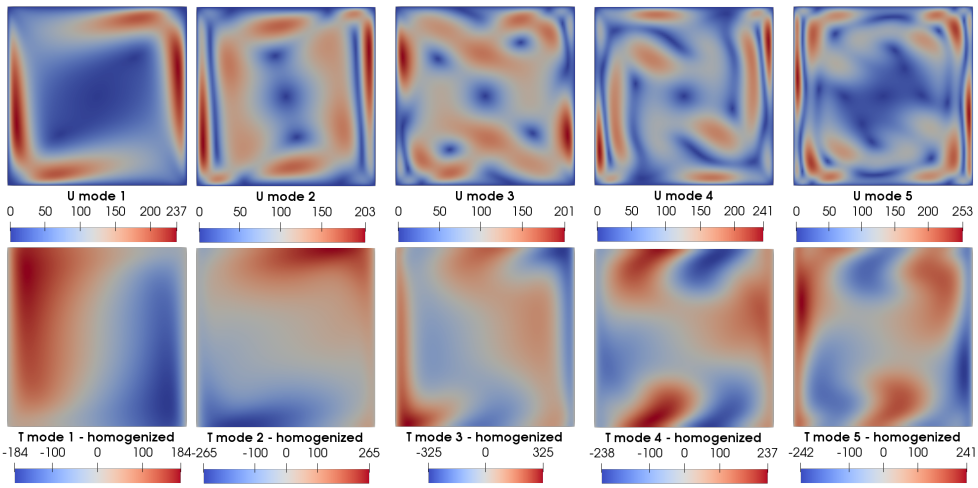

FIGURE 4. First 5 POD modes for velocity (top) and temperature with homogeneous BCs (bottom).

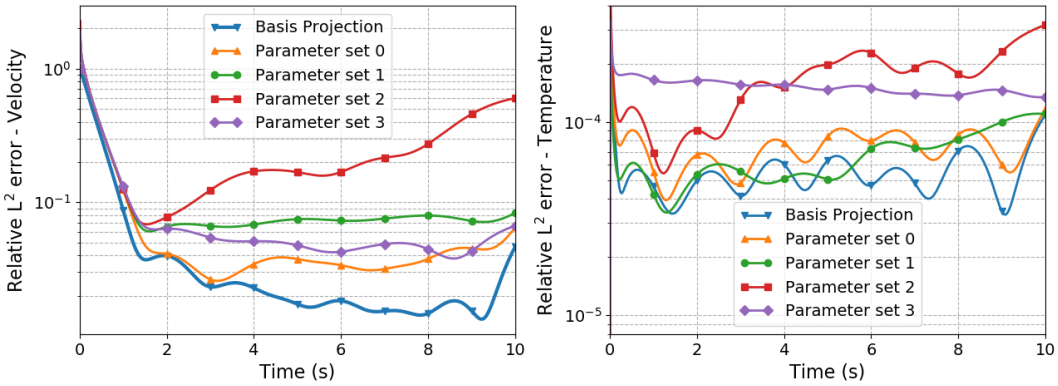

FIGURE 5. Relative L^2-error of velocity (left) and temperature (right) between the ROM with control function and the FOM for all parameter sets and the basis projection.

For parameter set 0, the L^2-prediction errors are of the same order as its basis projection error using 7 modes for both velocity and temperature. The velocity error is more than 1 at the beginning of the ROM simulation, as the flow starts at rest and therefore a small deviation of the initial velocity field leads to a high relative error as the error is magnified by a small velocity magnitude [8]. After about 1 second of simulation time the L^2-error of the velocity is less than 10^{-1} and for temperature below 10^{-4}. As expected, the performance of the ROM velocity is best when tested for the same parameter set on which the POD has been performed, but increases for each of

the following sets. For parameter set 1 and 3, after 2 seconds of simulation time, the error remains of the same order. However, the error of parameter set 3 keeps increasing over time, meaning that the ROM is less stable for those values. The same applies to the relative error of the temperature fields, however at some moments in time the ROM performs better for parameter set 1, where the temperature difference between the walls is smaller compared to set 0, than the basis projection. Then for parameter set 3, where an asymmetric temperature difference is applied on the walls, the ROM is stable, but performs worse than parameter set 1 due to the strong non-linearity of the flow with respect to the BCs. As no snapshots are collected for a similar case, part of the flow pattern is not contained in the snapshots and therefore also not in the ROM. The full order and reconstructed velocity and temperature fields for parameter set 3 are shown in Figure 6 at $t = 1$ s, $t = 5$ s and the final simulation time $t = 10$ s. The absolute error between the FOM and the ROMs is shown in the same figure, which is of the order 10^{-3} m/s for velocity and 10^{-2} K for temperature. Finally, the computation times on a single Intel Premium CPU G2130 @ 3.20GHz processor for calculating the FOM, POD modes, the reduced matrices and for the ROM are 563, 15, 0.5 and 27 seconds, respectively. Therefore, the ROM is about 20 times faster than the FOM.

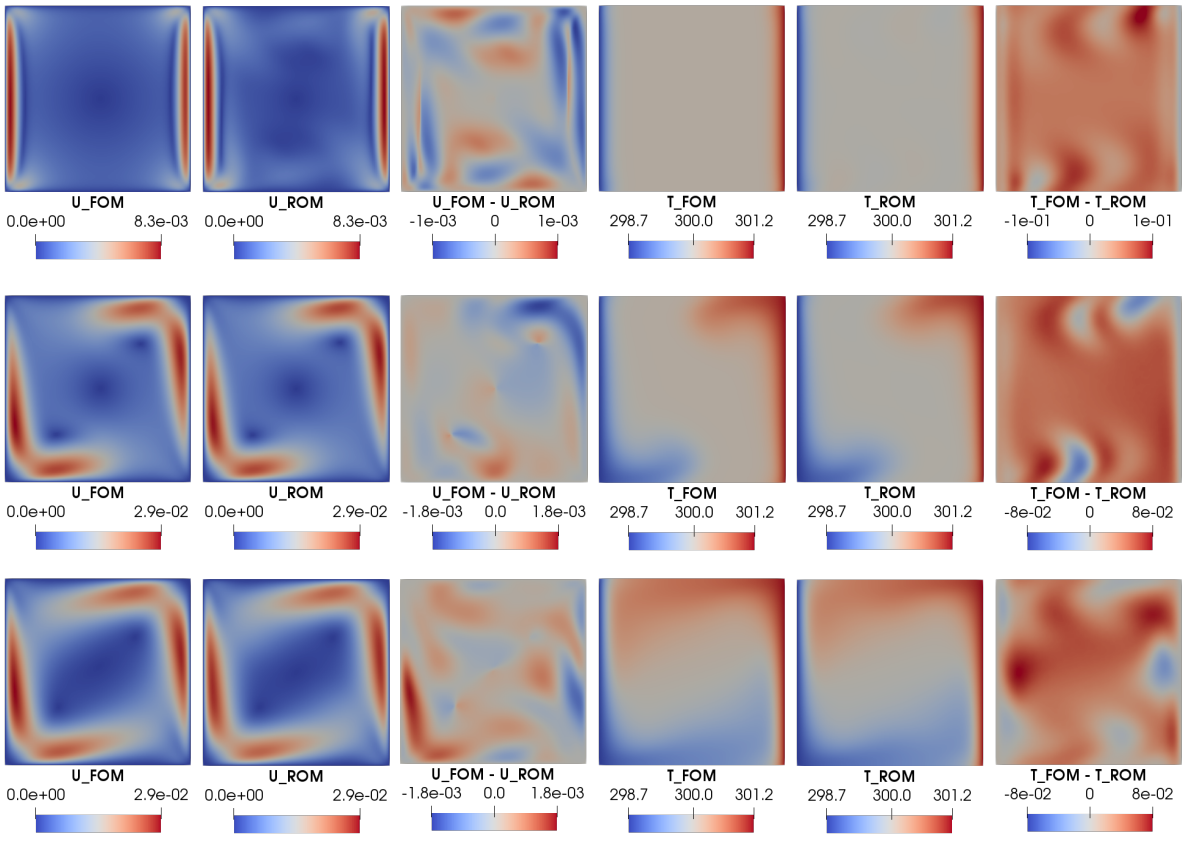

FIGURE 6. Comparison of the full order (FOM) velocity magnitude (1st column) and temperature (4th column) fields with the reduced order (ROM) fields (2nd and 5th column) and the difference between the FOM and ROM fields (3rd and 6th column) for parameter set 3 at t = 1 s (top), 5 s (middle) and 10 s (bottom).

7. Discussion

Only one full order solution for parameter set 0 was required to perform a ROM with the control function method for parameter set 1 and 3. However, the ROM is unstable for parameter set 2, even though the temperature BCs were only deviating by 0.5 K from those of set 0 (like parameter set 1), for which snapshots are collected. However, the temperature difference between the walls is larger for set 2 than the other sets for which the ROM is stable. As for larger temperature differences, part of the flow pattern is not contained in the snapshots, the ROM is not capable of reconstructing those fields. As a solution, when a larger range of parameter values needs to be tested, one can use snapshots from several FOMs to generate the POD modes. Since the POD modes are based on a linear combination of snapshots, while buoyancy driven flows are highly non-linear due to the coupling between the non-linear momentum and energy equations, adding snapshots from different FOMs can make the ROM applicable for a larger range of parameter values.

The relative L^2 error for velocity during the first second of the ROM simulation is about one order higher compared to the rest of the simulation. Especially for velocity, the error is more than 1 at the beginning of the ROM simulation. A small deviation of the homogeneous initial field, even for the basis projection using a reduced number of modes leads to a high relative error compared with the full order solution. The absolute error is of a smaller order, as shown by the absolute difference plot between the FOM and ROM fields at different time instances, and so, depending on the application, the error can be acceptable. Adding more modes to the reduced basis will reduce the error, but then the ROM will become slower and therefore there is a trade-off between the two.

The control function method is not solely meant for parameterizing the temperature BCs. Using non-homogeneous modes for the reduced basis construction can lead to an unstable ROM solution as the basis functions, and in the same way their BCs, are a linear combination of the snapshots [8]. The advantage of the control function method is that the functions can be determined on beforehand. However, not every function will lead to a stable ROM. Moreover, the output of the ROM can differ depending on which function is used and therefore extensive testing of ROMs for different functions could be needed. Best is to choose a function that is as close as possible to the full order problem. The control function is therefore physics based unlike, for instance, a penalty factor, which is an arbitrary value [7, 8]. For this case, solving a Laplacian function is an appropriate choice as no forced convection is applied to the problem. Lastly it is pointed out in literature [7] that long-time integration and initial condition issues can be more problematic for the control function method compared to the penalty method. However, this must be tested in a further research.

In this study, the recovery of the pressure has not been incorporated in the ROM. A supremizer enrichment of the velocity space technique or exploitation of a pressure Poisson equation can, for instance, be incorporated in the Galerkin projection to include the pressure in the ROM [5].

Finally, simulations have only been performed for air flow, as special attention is required to low Prandtl number thermal-hydraulics when modeling liquid metal flows.

8. Conclusions

In this paper, a FV-based POD-Galerkin ROM with Boussinesq approximation is presented. The ROM is constructed such that it is consistent with the FOM and both

velocity and temperature fields are considered. The reconstruction of the pressure field is, however, not considered as only enclosed flows are investigated in this study. An additional buoyancy term in the ROM induces a two-way coupling between momentum and energy, that is required for buoyancy modeling for nuclear thermal-hydraulic studies and other related industrial problems. A ROM is constructed of which the temperature BCs are parametrized using a control function method. The results of the ROMs for a simple 2D differentially heated cavity show that the relative error of temperature is of the order of 10^{-4} and of velocity 10^{-1} for the vast part of the simulations. The ROMs are stable, except when the temperature difference between the walls is larger than the case for which the snapshots, for the reduced basis construction, are collected. The accuracy can be improved by adding more modes to the reduced basis obtained with the POD method. Finally, the ROM is about 20 times faster than the FOM run on a single processor.
For further development, the pressure will be included in the ROM and the model will be extended for turbulent buoyant flows, which will be essential to simulate buoyancy in nuclear reactors.

9. Acknowledgements

This work has been partially supported by the ENEN+ project that has received funding from the Euratom research and training Work Programme 2016 - 2017 - 1 #755576.

References

[1] A. Toti, J. Vierendeels, and F. Belloni, "Coupled system thermal-hydraulic/cfd analysis of a protected loss of flow transient in the myrrha reactor," *Annals of Nuclear Energy*, vol. 118, pp. 199–211, 2018.

[2] S. Georgaka, G. Stabile, G. Rozza, and M. J. Bluck, "Parametric pod-galerkin model order reduction for unsteady-state heat transfer problems," *arXiv preprint: 1808.05175*, 2018.

[3] J. Weller, E. Lombardi, M. Bergmann, and A. Iollo, "Numerical methods for low-order modeling of fluid flows based on POD," *International Journal for Numerical Methods in Fluids*, vol. 63, no. 2, pp. 249–268, 2010.

[4] G. Stabile, S. Hijazi, A. Mola, S. Lorenzi, and G. Rozza, "POD-Galerkin reduced order methods for CFD using finite volume discretisation: vortex shedding around a circular cylinder," *Communications in Applied and Industrial Mathematics*, vol. 8, no. 1, pp. 210–236, 2017.

[5] G. Stabile and G. Rozza, "Finite volume POD-Galerkin stabilised reduced order methods for the parametrised incompressible navier–stokes equations," *Computers & Fluids*, vol. 173, pp. 273–284, 2018.

[6] A. Quarteroni, G. Rozza, *et al.*, *Reduced order methods for modeling and computational reduction*, vol. 9. Springer, 2014.

[7] W. Graham, J. Peraire, and K. Tang, "Optimal control of vortex shedding using low-order models. part i - open-loop model development," *International Journal for Numerical Methods in Engineering*, vol. 44, no. 7, pp. 945–972, 1999.

[8] L. Lorenzi, A. Cammi, L. Luzzi, and G. Rozza, "POD-galerkin method for finite volume approximation of Navier-Stokes and RANS equations.," *Comput. Methods Appl. Mech. Engrg*, vol. 311, 2016.

[9] H. Jasak, A. Jemcov, and Ž. Tuković, "Openfoam: A c++ library for complex physics simulations," Intl. workshop on coupled methods in numerical dynamics, Croatia, 2007.

[10] F. Moukalled, L. Mangani, M. Darwish, *et al.*, "The finite volume method in computational fluid dynamics," *An Advanced Introduction with OpenFOAM and Matlab*, pp. 3–8, 2016.

[11] G. Stabile and G. Rozza, "Ithaca-fv - in real time highly advanced computational applications for finite volumes." www.mathlab.sissa.it/ithaca-fv. Accessed: 2018-11-26.